

Magnetic imaging of ion-irradiation patterned Co/Pt multilayers using complementary electron and photon probes

G. J. Kusinski,^{a),b)} K. M. Krishnan, G. Denbeaux, and G. Thomas^{b)}

Materials Sciences Division, Lawrence Berkeley National Laboratory, Berkeley, California 94720

B. D. Terris and D. Weller^{c)}

IBM Almaden Research Center, 650 Harry Road, San Jose, California 95120

(Received 2 April 2001; accepted for publication 30 July 2001)

The three-dimensional magnetic structure and reversal mechanism of patterned Co/Pt multilayers, were imaged using complementary Lorentz transmission electron microscopy (in-plane component) and magnetic transmission x-ray microscopy (perpendicular magnetization). The Co/Pt films with perpendicular anisotropy were patterned by ion irradiation through a stencil mask to produce in-plane magnetization in the irradiated regions. The boundaries of the patterns, defined by the transition from out-of-plane to in-plane magnetization, were found to be determined by the stencil mask. The nucleation fields were substantially reduced to 50 Oe for the in-plane regions and 1 kOe for the perpendicular regions, comparing to 4.5 kOe for the as-grown film. The perpendicular reversals were found to always originate at the pattern boundaries. © 2001 American Institute of Physics. [DOI: 10.1063/1.1407301]

Understanding the magnetic reversal mechanism in thin films is of both scientific and technological importance. Conventional magnetometry measurements are limited to detecting averaged magnetic properties and can not give direct information about local nucleation events or reversal mechanisms. Hence, the development of magnetic imaging techniques, capable of detecting the onset of isolated nucleation events and imaging the progress of the magnetic reversal on the local scale, are a key to a comprehensive understanding of the magnetization phenomena. This is particularly important in studies of patterned magnetic media, where the magnetic structure is spatially confined or modified by various lithographical techniques.^{1,2} A specific example is the Co/Pt multilayer (ML) structure with perpendicular anisotropy, arising from interface and strain effects,³ which can be systematically reduced by ion beam irradiation. At sufficiently high doses, the easy magnetization axis is rotated from out of plane to in plane.^{4,5} It has been shown that using resist⁶ or stencil masks⁷ to spatially vary the dose of ions incident on the film, or by utilizing focussed ion beam writing,⁸ patterns of in-plane and out-of-plane magnetization can be produced. Such direct modification of the magnetic properties on the local scale may be useful for future high-density patterned magnetic data storage. One important aspect of this patterning technique is the nature of the magnetic interaction between the irradiated, (in-plane regions), and the nonirradiated matrix regions with perpendicular anisotropy. Particularly important is how the switching fields and the reversal mechanisms in one region are influenced by the other. To study

such effects, it is essential to investigate the three-dimensional magnetic structure using high-resolution magnetic imaging techniques.

In this letter, studies of the magnetic reversal processes of magnetic arrays fabricated by the ion beam irradiation of Co/Pt MLs are reported. For our studies, we chose two complementary magnetic imaging techniques, Lorentz transmission electron microscopy (LTEM)⁹ sensitive to in-plane magnetization and magnetic transmission x-ray microscopy (M-TXM)¹⁰ measuring perpendicular magnetization.¹¹ The Co/Pt multilayers, 20 nm Pt/10×(0.3–0.4 nm Co/1 nm Pt)/2 nm Pt with perpendicular anisotropy, were grown on electron transparent SiN windows by electron beam evaporation at a growth temperature $T_G \cong 250^\circ\text{C}$.⁵ Magneto-optical Kerr effect (MOKE) hysteresis measurements were performed for the as-grown ML. A rectangular MOKE loop, Figure 1(a), shows perpendicular easy direction of magnetization with coercivity $H_{C\perp} = 6.8\text{ kOe}$. The physical microstructure of the films was characterized by transmission electron microscopy (TEM) and high-resolution TEM.¹² The magnetic patterns, consisting of 1.4 μm dots with in-plane anisotropy within the perpendicular anisotropy matrix, were created by irradiation with 700 keV N^+ ions through a stencil mask,⁷ without changing the topography of the sample. The irradiation dose and ion species were selected to give in-plane magnetization in the irradiated regions.⁵ By using such a well-defined magnetic pattern, we are able to image the interactions between in-plane and out-of-plane regions. A series of Fresnel LTEM images of the patterned MLs were recorded during the *in situ* magnetizing experiment using a weakly excited objective lens and tilting the sample to apply an in-plane field.¹³ At the M-TXM remanent states were imaged after applying polar magnetic fields (H_{\perp}) of varying magnitudes between 14 and -14 kOe . The incident photon energy was tuned to the Co L_3 absorption edge was tuned and magnetic structure was imaged with a 25

^{a)}Electronic mail: kusinski@uclink4.berkeley.edu

^{b)}Also at: Materials Science Division, Lawrence Berkeley National Laboratory, Berkeley, California 94720.

^{c)}Current address: Seagate Technology, 2403 Sidney Street, Pittsburgh, Pennsylvania 15203.

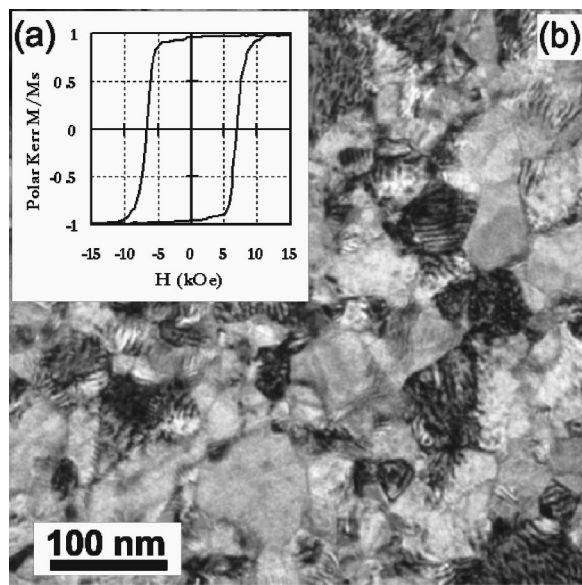


FIG. 1. (a) Normalized MOKE hysteresis loop of as-grown Co/Pt multilayer is shown. (b) Bright field TEM image, note 20–100 nm grain size.

nm spatial resolution with contrast provided by x-ray magnetic circular dichroism.

Selected LTEM images summarizing the in-plane magnetization reversal processes are shown in Fig. 2. The circular patterns shown on the image are the ion-irradiated regions. An in-plane field of $H_{\parallel}=264$ Oe, Fig. 2(a), was sufficient to magnetically align all the irradiated areas. The Fresnel contrast consists of bright (top) and dark (bottom) fringes for each irradiated pattern, consistent with these regions being magnetized in-plane to the left-hand side, along the applied field direction.¹⁴ The nonirradiated matrix was not affected by the applied field and was still magnetized in the polar direction. The small contrast variations in these areas are due to the physical microstructure, which is shown at a larger magnification in Fig. 1(b). When the in-plane field was reversed, magnetic switching of the bits was recorded

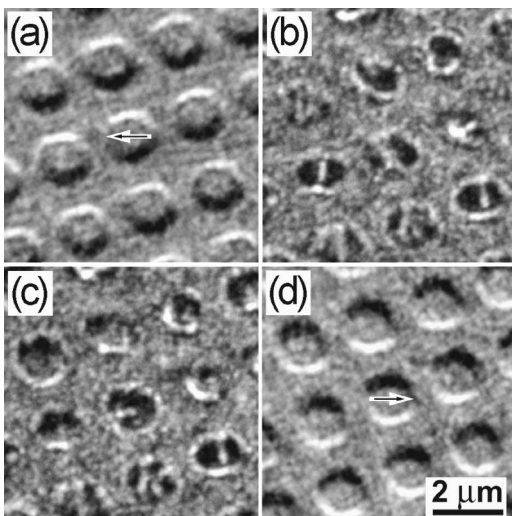


FIG. 2. Fresnel images of the patterned multilayers, recorded during *in situ* LTEM experiment are shown. (a) $H_{\parallel}=264$ Oe, (b) $H_{\parallel}=-67$ Oe, (c) $H_{\parallel}=-93$ Oe, and (d) $H_{\parallel}=-264$ Oe. Arrows indicate the direction of magnetization. Notice the same location of the domain wall in bottom-right-hand side bit in images (b) and (c).

with nucleation at approximately $H_{\parallel}=-50$ Oe, and subsequent domain wall motion between pinning centers. Figure 2(b), recorded at $H_{\parallel}=-67$ Oe, shows domain walls pinned at a various location within each of the bits. At larger negative fields [Fig. 2(c), $H_{\parallel}=-93$ Oe], further domain wall jumps were observed. However, for some of the bits, domain walls remained pinned in the same location as shown by the bit in the bottom right-hand side corner of Figs. 2(b) and 2(c). Applying $H_{\parallel}=-264$ Oe, Fig. 2(d), resulted in the complete reversal of the patterns. The ion irradiated, unmasked areas were thus confirmed to have in-plane magnetization.

On the other hand, the M-TXM is sensitive to the out-of-plane component of the magnetization. In our setup, when the magnetization of the samples is in a positive (negative) polar direction, it is antiparallel (parallel) to the x-ray polarization, resulting in increased (decreased) absorption and hence dark (bright) areas in the image. For the in-plane magnetized regions, regardless of the direction, the absorption is not affected and gives an intermediate uniform gray contrast.

The sample imaged after saturation at $H_{\perp}+14$ kOe, Fig. 3(a), showed contrast consistent with the irradiation pattern. The nonirradiated matrix has uniform dark contrast, demonstrating uniform, positive, polar magnetization. The LTEM results, showing the irradiated regions to be magnetized in plane were used to interpret the M-TXM images. With no in-plane field applied, LTEM analysis found a multidomain configuration for each of the regions. However, the M-TXM technique has no sensitivity to the in-plane orientation of the magnetization, hence, uniform intensity within each irradiated area is expected. After saturation in the opposite direction with $H_{\perp}=-14$ kOe, Fig. 3(b), the unirradiated matrix showed a uniform bright contrast, consistent with a perpendicular negative magnetization. Line profiles obtained from the areas labeled with rectangles in Figs. 3(a) and 3(b) are shown in Figs. 3(c) and 3(d), respectively. The normalized intensity levels across the ion-irradiated circles were the same, and were equal to the average between that of positive and negative polar magnetization. At $H_{\perp}+1$ kOe, Fig. 3(e), early stages of the nucleation of positive domains were recorded near the edges of the irradiated patterns, as shown by the black contrast. When increasingly larger fields were applied [Fig. 3(f), $H_{\perp}+3$ kOe], the interface regions reversed first, and a continuous reversed area was observed around the circumference of each circle before the domain wall propagated substantially into the matrix. Application of larger fields [Fig. 3(g), $H_{\perp}+4$ kOe] resulted in a radial growth of the reversed domains away from the irradiated areas. The propagation of the domain wall into the unirradiated regions was characterized by a jagged structure. Only at $+4$ kOe $< H_{\perp} < +5$ kOe, nucleation of the reversed “black” domains away from the edge of the irradiated pattern was first observed. This is consistent with the nucleation field measured from the magnetic hysteresis loop ($H_n \sim 4$ kOe) of the as-grown nonpatterned film. Figure 3(h) shows a few isolated ~ 100 nm reversed domains; at this point, the domains nucleated at the edges extend up to 200 nm from the pattern edge. This suggests that ion irradiation introduced low field nucleation centers at pattern boundaries.^{4,8} Above $H_{\perp}+5$ kOe, further nucleation events and growth of all domains was observed. At $H_{\perp}+$

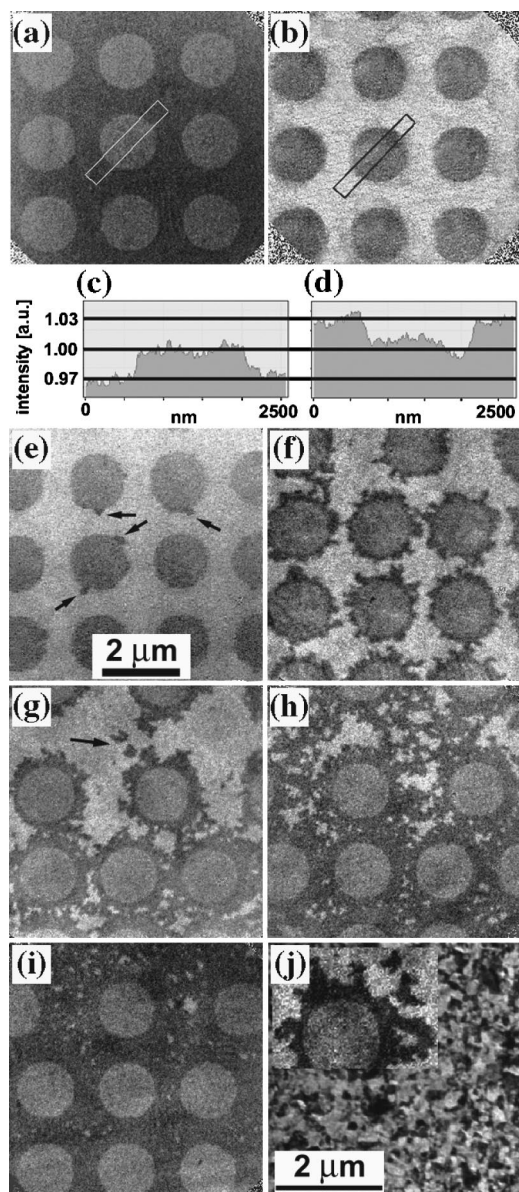


FIG. 3. M-TXM images of the patterned Co/Pt multilayers taken at the Co L_3 absorption edge. (a) $H_{\perp} = +14$ kOe, (b) $H_{\perp} = -14$ kOe, (c), and (d) normalized line profiles obtained from the areas labeled with rectangles on images (a) and (b) respectively. (e) Onset of nucleation at the edges of irradiated patterns, $H_{\perp} = +1$ kOe, (f) $H_{\perp} = +3$ kOe, (g) $H_{\perp} = +4$ kOe, (h) $H_{\perp} = +5$ kOe, (i) $H_{\perp} = +7$ kOe, and (j) Magnetic image at $H_{\perp} = +4$ kOe are superimposed on the TEM at the same magnification.

+7 kOe, which is higher than the coercive field of the non-irradiated sample, the majority of the matrix was reversed; however, small unreversed (bright) areas were still observed, Fig. 3(i). In agreement with the magnetic measurements, fields of +10 kOe were necessary to fully saturate the matrix. An x-ray image of the same sample location recorded using photons off the Co absorption edge showed no contrast indicating uniform sample thickness. Hence, the contrast in the M-TXM images in Fig. 3 is only magnetic without any topographic contribution.

The absence of thickness variation was confirmed by TEM investigation, which, in addition, found columnar grain structure, 20 ± 50 nm Fig. 1(b). A magnetic image at $H_{\perp} = +4$ kOe superimposed on the TEM image, Fig. 3(j),

showed the roughness of the reversed domains to be similar to the physical microstructure. This suggests that the microstructure influences both the domain wall pinning and the reversal processes.^{15,16}

In summary, the unique combination of LTEM and M-TXM allowed us to image the three-dimensional magnetization structure of the patterned film. The boundaries of the patterns, defined by the transition from out-of-plane to in-plane magnetization, were found to be determined by the stencil mask, while the scale of the magnetic reversal was governed by the grain size. The ion-irradiated circular regions, were magnetically soft with saturation below 300 Oe, and had in-plane easy axis of magnetization. The reversal in the nonirradiated matrix, exhibiting perpendicular anisotropy, was by nucleation of reversed domains at the pattern boundaries followed by domain wall motion in the nonirradiated region. These nucleation fields, $Hn_{\perp} = 1$ kOe, were significantly lower than nucleation fields for the as-grown film $Hn_{\perp}^0 \cong 4$ to 5 kOe.

One of the authors (G.K.) acknowledges financial support through the "IBM Research Fellowship." Work at NCEM/LBNL was supported by the U.S. Department of Energy under Contract No. DE-AC03-76SF00098. The authors thank A. Kellock and J. E. E. Baglin for ion-irradiation support and E. C. Nelson for assistance on the CM200/FEG.

¹M. Farhoud, M. Hwang, H. I. Smith, M. L. Schattenburg, J. M. Bae, K. Youcef-Toumi, and C. A. Ross, *IEEE Trans. Magn.* **34**, 1087 (1998).

²C. A. Ross, H. I. Smith, T. Savas, M. Schattenburg, M. Farhoud, M. Hwang, M. Walsh, M. C. Abraham, and R. J. Ram, *J. Vac. Sci. Technol. B* **17**, 3168 (1999).

³B. Zhang, K. M. Krishnan, C. H. Lee, and R. F. C. Farrow, *J. Appl. Phys.* **73**, 6198 (1993).

⁴J. Ferre, C. Chappert, H. Bernas, J.-P. Jamet, P. Meyer, O. Kaitasov, S. Lemerle, V. Mathet, F. Rousseaux, and H. Launois, *J. Magn. Mater.* **191**, 198 (1999).

⁵D. Weller, J. E. E. Baglin, A. J. Kellock, K. A. Hannibal, M. F. Toney, G. Kusinski, S. Lang, L. Folks, M. E. Best, and B. D. Terris, *J. Appl. Phys.* **87**, 5768 (2000).

⁶C. Chappert, H. Bernas, J. Ferre, V. Kottler, J.-P. Jamet, Y. Chen, E. Cambril, T. Devolder, F. Rousseaux, V. Mathet, and H. Launois, *Science* **280**, 1919 (1998).

⁷B. D. Terris, L. Folks, D. Weller, J. E. E. Baglin, A. J. Kellock, H. Rothuizen, and P. Vettiger, *Appl. Phys. Lett.* **75**, 403 (1999).

⁸T. Aign, P. Meyer, S. Lemerle, J. P. Jamet, J. Ferre, V. Mathet, C. Chappert, J. Gierak, C. Vieu, F. Rousseaux, H. Launois, and H. Bernas, *Phys. Rev. Lett.* **81**, 5656 (1998).

⁹J. N. Chapman and M. R. Scheinfein, *J. Magn. Mater.* **200**, 729 (1999).

¹⁰G. Denbeaux, P. Fischer, G. Kusinski, M. Le Gros, A. Pearson, and D. Attwood, *IEEE Trans. Magn.* **37** 2764 (2001).

¹¹M-TXM is implemented at the beam line 6.1.2 of the Advanced Light Source at Lawrence Berkeley National Laboratory.

¹²G. J. Kusinski, (unpublished).

¹³G. J. Kusinski, K. M. Krishnan, D. Weller, B. D. Terris, L. Folks, A. J. Kellock, J. E. E. Baglin, and G. Thomas, in *Conference Proceedings of Magnetic Storage Systems Beyond 2000*, edited by G. Hadjipanayis (Kluwer Academic Publishers) (unpublished).

¹⁴The electron beam deflection is perpendicular to the direction of magnetization according to the Lorentz force. The uniformly magnetized region yields an increased intensity at one end and decreased intensity at the other end. The multidomain configuration yields a contrast consisting of bright and dark lines (domain walls) within the region. (see Ref. 9)

¹⁵D. Weller, L. Folks, M. Best, E. E. Fullerton, B. D. Terris, G. J. Kusinski, K. M. Krishnan, and G. Thomas, *J. Appl. Phys.* **89**, 7525 (2001).

¹⁶S. Lemerle, J. Ferre, C. Chappert, V. Mathet, T. Giamarchi, and P. LeDoussal, *Phys. Rev. Lett.* **80**, 849 (1998).